Astron. Astrophys. 333, 926–941 (1998)

ASTRONOMY AND ASTROPHYSICS

The puzzling MgAl anticorrelation in globular-cluster red giants: primordial plus deep mixing scenario?

P.A. Denissenkov[1,2,3], **G.S. Da Costa**[1], **J.E. Norris**[1], **and A. Weiss**[3]

[1] Mount Stromlo and Siding Spring Observatories, Institute of Advanced Studies, The Australian National University, Private Bag, Weston Creek P.O., ACT 2611, Australia
[2] Astronomical Institute of the St. Petersburg University, Bibliotechnaja Pl. 2, Petrodvorets, 198904 St. Petersburg, Russia
[3] Max-Planck-Institut für Astrophysik, Karl-Schwarzschild-Strasse 1, D-85740 Garching, Germany

Received 22 July 1997 / Accepted 26 November 1997

Abstract. Star-to-star abundance variations of C, N, O, Na and Al in globular-cluster red giants have been recently supplemented by the finding that [Mg/Fe] is depleted in stars with extremely large [Al/Fe] (Shetrone 1996a). To find out which of the magnesium isotopes is responsible for the observed depletion of [Mg/Fe] Shetrone (1996b) also undertook an isotopic analysis of Mg and found that it is ^{24}Mg which is depleted in Al-rich giants. On the other hand, Norris & Da Costa (1995) demonstrated that even in the massive globular cluster ω Cen which has intrinsic spreads in both [Fe/H] and the abundances of the s-process elements, [O/Fe] anticorrelates with [Na/Fe] and [Al/Fe] as in "normal" monometallic clusters. These new spectroscopic results allow us to test current models of stellar evolution and nucleosynthesis, as well as those of the formation and chemical enrichment of globular clusters. In an effort to explain self-consistently these observations we have considered two possibilities: (1) a deep mixing scenario which assumes that in red giants some kind of (extra)mixing transports products of nuclear reactions from the hydrogen burning shell (HBS) to the base of the convective envelope; and (2) a combination of primordial and deep mixing scenarios. It is shown that (1) cannot account for the anticorrelation of [Mg/Fe] vs. [Al/Fe] without additional *ad hoc* assumptions, among which we identify a strong but still undetected low energy resonance in the reaction ^{24}Mg(p,γ)^{25}Al, and episodical increases of the HBS temperature up to the value $T \approx 74\,10^6$ K. In (2) intermediate mass AGB stars are assumed to produce the decreased ^{24}Mg and increased ^{25}Mg initial abundances in some globular-cluster low mass stars and Al is synthesized at the expense of ^{25}Mg in the HBS and transported to the surface of the red giant by extramixing. We discuss advantages and deficiencies of both scenarios and propose some observational tests.

Key words: stars: abundances – stars: evolution – stars: interiors – globular clusters: general

1. Introduction

Recently Shetrone (1996b, hereafter S96) has determined magnesium isotopic compositions for a small sample of bright red giants in the globular cluster M 13. His finding that many giants in this system have [(^{25}Mg+^{26}Mg)/^{24}Mg] $\sim$ +0.4, in stark contrast to values $\sim$ –0.4 found in field halo stars (see also McWilliam & Lambert 1988 and references therein), is of fundamental importance, and highlights yet again the differences in abundance patterns found in cluster and field stars. Shetrone's work followed the earlier discovery that large Al enhancements were usually accompanied by moderate Mg depletions in this cluster (Shetrone 1996a), as well the demonstration that anticorrelations of Na and Al with O exist not only in "normal" monometallic clusters such as M 13 (see Kraft et al. 1997) but also in the massive globular cluster ω Cen whose stars show intrinsic spreads in both metallicity and the abundances of the s-process elements (Norris & Da Costa (1995, hereafter ND95)). These new data challenge stellar evolution theory to provide an appropriate explanation of the abundance anomalies, on the one hand, and present a number of new observational constraints on possible primordial processes responsible for abundance variations in globular clusters, on the other. In this paper we use the latest spectroscopic results to address the question of whether the modern theory of nucleosynthesis in stars can self-consistently reproduce the whole spectrum of abundance variations seen in globular-cluster red giants (GCRGs) and, if not, to seek constraints on additional *ad hoc* assumptions which make such reproduction possible.

Stars leaving the main sequence (MS) in present-day globular clusters have small masses $M \approx 0.8 - 0.9\,M_\odot$ and very low metallicities, covering the range –2.4 < [Fe/H] < –0.2, corresponding to $8\,10^{-5} <$ Z < 0.01, (where we adopt [Fe/H] = $lg(Z/Z_\odot)$, and $Z_\odot = 0.01886$ (Anders & Grevesse 1989))[1]. Standard stellar evolution theory has no doubts about subsequent structural and chemical histories of such stars, at least

Send offprint requests to: A. Weiss (weiss@mpa-garching.mpg.de)

[1] We use the standard spectroscopic notation, i.e. [A/B]= $\lg(N(\mathrm{A})/N(\mathrm{B}))_{\mathrm{star}} - \lg(N(\mathrm{A})/N(\mathrm{B}))_\odot$, where N(A) and N(B) are atomic number densities of the nuclides A and B, respectively. Z is the mass fraction of elements heavier than helium.

until the beginning of the core helium flash. MS central hydrogen burning, which was dominated by pp-chains, is now replaced by shell hydrogen burning with the main energy output provided by the CNO-cycle. The shell advancing outwards in mass causes a gradual growth of the underlying helium core until the core mass becomes large enough to trigger the helium flash. These internal structural changes are accompanied by the star ascending the red giant branch (RGB). Its surface chemical composition is not expected to change significantly during this evolutionary stage. The only important event between the MS turn-off and the core helium flash is the well-known first dredge-up episode which takes place on the subgiant branch. The displacement of the star from the MS to a cooler region of the HR diagram favours the convective envelope extending its base into deep layers which were in radiative equilibrium on the MS and where some mild transformations among CN isotopes in the then energetically unimportant CN-cycle occurred. As a result the surface abundances of ^{12}C, ^{13}C and ^{14}N (as well as those of ^{7}Li, ^{3}He and a few other light nuclides which are not discussed in this work; for recent theoretical results on their standard dredge-up and non-standard deep mixing evolutionary changes see Sackmann & Boothroyd (1997), Weiss et al. (1996) and Charbonnel (1995)) begin to decline from their initial values. This excursion of the base of the convective envelope (BCE) into the interior of the star continues until it arrives at its deepest penetration, which corresponds to the end of the first dredge-up; after that, convection begins to retreat and later follows approximately the outward advancement of the hydrogen burning shell (HBS). Our standard evolutionary calculations for a $M = 0.8\,M_{\odot}$ star show that, depending on Z, the first dredge-up changes of the surface ^{12}C, ^{13}C and ^{14}N abundances are indeed very modest: $(Z, ^{12}\mathrm{C}/^{13}\mathrm{C}, \Delta\lg{}^{12}\mathrm{C}, \Delta\lg{}^{14}\mathrm{N})$ = $(10^{-4}, 64, -0.0024, 0.0025)$, $(5\,10^{-4}, 50, -0.0064, 0.012)$, $(5\,10^{-3}, 45, -0.0092, 0.021)$ (on the MS ^{12}C/^{13}C≈ 90; here and in what follows a nuclide's chemical symbol is used also to denote its number density).

When comparing these predictions of standard stellar evolution theory with available observational data on the atmospheric chemical composition of red giants in globular clusters one finds obvious and numerous disagreements. *(i)* The measured ^{12}C/^{13}C ratios have very low values often approaching the limit 3.5 which is a characteristic of the equilibrium CN-cycle (Smith & Suntzeff 1989; Brown & Wallerstein 1989; Suntzeff & Smith 1991; Brown et al. 1991a; Briley et al. 1994; S96). *(ii)* The differences in C and N among red giants in the same cluster reach an order of magnitude or even more. Moreover, carbon abundances [C/Fe] are found to anticorrelate with luminosity (to correlate with the absolute visual magnitude), consistent with a progressive C depletion as the star ascends the RGB at luminosities well above the end of the canonical first dredge-up (as seen, for example, in M 92 and NGC 6397 (Bell et al. 1979; Langer et al. 1986; Briley et al. 1990), M 4 and NGC 6752 (Suntzeff & Smith 1991)). *(iii)* The most intriguing result is that in many globular clusters there are large (up to 1 dex) variations of O and Na among red giants (Kraft 1994) and in some clusters Al and Mg abundances also vary from star to star (Kraft et al. 1997).

It is important to note that all nuclides mentioned above whose abundances show considerable scatter in GCRGs (^{12}C, ^{13}C, N, O, Na, Mg isotopes and Al) are potential participants in hydrostatic hydrogen burning. During transformation of H into He in the CNO-cycle, which plays the chief role in this process, the relative abundances of the CNO nuclides are changing whereas their net sum remains constant, i.e. the CNO nuclides actually work as catalysts. So do the NeNa and MgAl nuclides in the NeNa- and MgAl-cycles, respectively. Detailed flow-charts and the latest estimates of reaction rates for all three cycles can be found in the review of Arnould et al. (1995). Such approximate constancy of the sum C+N+O, despite the large spreads in the individual abundances of C, N and O, has been observed in M 13 and M 3 by Smith et al. (1996), in NGC 362 and NGC 288 by Dickens et al. (1991) and in ω Cen by ND95. There is also some evidence of constancy of the sum Mg+Al in M 13 (Kraft et al. 1997).

In contradistinction, the heavier α elements such as Si, Ca and Ti, which are believed to be produced by successive α-captures in massive stars and which do not participate in hydrostatic hydrogen burning, do not show any scatter in GCRGs. Instead their mean abundances agree well with the abundances of α-elements observed in field Population II dwarfs, i.e. $\langle[\alpha/\mathrm{Fe}]\rangle \approx +0.4$. In addition, the iron peak elements Cr and Ni, synthesized during SNe explosions, do not exhibit abundance anomalies. As regards Fe itself, in most globular clusters its abundance is surprisingly constant within the same cluster. The only exception of the rule is ω Cen (M 22 may be another) where the abundance range $-1.8 <$[Fe/H]< -0.8 and the rise of abundances of s-process elements with that of Fe are certainly records of the cluster's more complicated chemical enrichment history (ND95).

To summarize, observations strongly support the idea that the star-to-star abundance variations (or, more precisely, at least a substantial part of them) in globular clusters were presumably produced during hydrogen burning. The fact that there are fairly good correlations between overabundances of N, Na and Al, on the one hand, and underabundances of C, O and Mg, on the other hand, is undoubtedly a sign of these abundance anomalies' simultaneous origin. The next question to answer is the place where these variations were produced. In our attempt to solve this puzzle we have chosen the latest spectroscopic data on the chemical composition of red giants in the globular clusters M 13 (Kraft et al. 1997; S96) and ω Cen (ND95). The former cluster is an extreme representative of "normal" (i.e. showing neither iron nor neutron-rich elements abundance variations) which contributes much to the "global anticorrelation" of [O/Fe] versus [Na/Fe] (see the review paper by Kraft 1994). ω Cen, on the other hand, provides evidence that the O vs. Na and O vs. Al anticorrelations are not a prerogative of "normal" clusters. Furthermore, ω Cen is the only globular cluster not obeying the "global anticorrelation" since it contains giants with extremely high [Na/Fe] (up to 1 dex) well above the general trend seen in "normal" clusters where [Na/Fe] saturates at ~ 0.5 dex. We shall see how theory can interpret this anomaly.

It should be noted that the standard stellar evolution theory fails to predict the low $^{12}C/^{13}C$ ratios seen in Population I giants of mass $\lesssim 2M_{\odot}$, too (Gilroy & Brown 1991; Charbonnel 1994). So, globular clusters are not unique in this regard. It is important to point out, however, that in GCRGs the number of nuclides whose abundances are known to vary from star to star is larger and the abundance variations themselves are more pronounced than in Population I giants.

The remainder of the paper is organized as follows. In Sect. 2 we briefly describe our theoretical tools – computer codes used to perform stellar evolution and nucleosynthesis calculations. Sect. 3 deals with the most promising candidate for the origin of the star-to-star abundance variations in globular clusters – deep mixing in evolving red giants. This, however, provides an incomplete solution to the problem. Sources of additional primordial pollution (SNe explosions, AGB stars and a "black box") which can contribute and modify the deep mixing scenario are discussed in Sect. 4. (We refer the reader also to Smith & Kraft (1996) who suggest that Ne novae may provide the additional pollution. In the present work we shall not address this possibility.) Our concluding remarks are given in Sect. 5.

2. Computer codes used in the paper

To calculate the evolution of a $M = 0.8\,M_{\odot}$ star from the ZAMS through to the core helium flash we used the code described by Raffelt & Weiss (1992), which, in the meantime, has been updated with respect to new opacity data (Rogers & Iglesias 1992; Iglesias & Rogers 1996) and plasma neutrino emission (Haft et al. 1994). The mass fraction of heavy elements was taken as $Z = 5\,10^{-4}$ ($\lg Z/Z_{\odot} = -1.58$) to approximately match the metallicities of M 13 ([Fe/H] = –1.49) and ω Cen ($-1.8 <$[Fe/H]< -0.8), whereas the initial helium abundance was $Y = 0.24$ as in the big bang composition (Walker et al. 1991). The adopted value of the mixing length parameter $\alpha = 1.48$ (times the pressure scale height, H_P) came from calibrating a solar model.

A number of selected red giant models were used to interpolate temperature and density distributions as well as to follow the movements in mass of the HBS and the BCE as the star ascends the RGB. Following the procedures described in Denissenkov & Weiss 1996 (Paper I), mixing in the radiative zone between the HBS and the BCE was modelled by introducing diffusion terms into the standard equations of nuclear kinetics. Results of these deep mixing calculations depend on a choice of two parameters: the depth of mixing $\delta M_{\rm mix}$ determined as a relative mass coordinate of the deepest radiative layer involved in the mixing (measured from the HBS in units of the mass separating the HBS and the BCE), and the diffusion coefficient $D_{\rm mix}$. The latter may not be chosen arbitrarily large because there are some estimates of its "reasonable" upper limit values which yield $D_{\rm mix}\sim 10^7 - 10^9\,{\rm cm^2\,s^{-1}}$ (see Paper I). The nuclear kinetics network used in the deep mixing calculations includes all important nuclides participating in the reactions of the CNO-, NeNa- and MgAl-cycles as well as those in a few reactions of the pp-chains (to follow changes of the ^{3}He abundance) and numbers 26 particles coupled by 30 reactions.

To estimate nucleosynthesis yields from intermediate mass AGB stars we employed an algorithm developed by Denissenkov et al. (1997, hereafter Paper II) which is very similar to the scheme used by Renzini & Voli (1981). The algorithm takes into account nuclear processing in the HBS (in an AGB star!) and at the BCE (hot bottom burning, hereafter HBB) between pulses as well as the convective shell He burning nucleosynthesis during a pulse in a simplified parameterized manner. A number of parameters are not well constrained in these calculations. For instance, the temperature of the HBB and the amount of material dredged up after finishing every pulse remain very uncertain (Lattanzio et al. 1997). Therefore, in Sect. 4 we shall concentrate only on those results of our nucleosynthesis calculations in intermediate mass AGB stars which weakly depend on the choice of such parameters or, otherwise, specially emphasize which values of parameters lead to a particular result supported by observations. Unfortunately, mainly because of uncertainties in the current treatment of convective overshoot in stars (Frost & Lattanzio 1996), such an approach seems to be the only one possible at present. Our nuclear kinetics network applied in AGB stars includes the same nuclides and reactions as those in the deep mixing code plus Si isotopes; 3α-reaction; (α,γ)-reactions on ^{12}C, ^{14}C, ^{14}N, ^{15}N, ^{16}O, ^{17}O, ^{18}O, ^{20}Ne, ^{21}Ne, ^{22}Ne, ^{24}Mg, ^{25}Mg and ^{26}Mg; $(\alpha$,n)-reactions on ^{13}C, ^{17}O, ^{18}O, ^{21}Ne, ^{22}Ne, ^{25}Mg and ^{26}Mg; neutron captures by ^{12}C, ^{13}C, ^{16}O, ^{19}F, ^{20}Ne, ^{21}Ne, ^{22}Ne, ^{23}Na, ^{24}Mg, ^{25}Mg, ^{26}Mg, ^{27}Al, ^{28}Si, ^{29}Si, ^{30}Si and by an averaged neutron-sink heavy "nucleus" $^{31}X_{14}$; as well as the reactions ^{14}C(p,γ)^{15}N, ^{14}N(n,p)^{14}C, ^{19}F(α,p)^{22}Ne, ^{26}Al$^{\rm g}$(n,p)^{26}Mg, ^{21}Ne(n,α)^{18}O and ^{26}Al$^{\rm g}$(n,α)^{23}Na. The total numbers of nuclides and reactions in this network are 26 and 69, respectively.

To check the degree to which the s-process nucleosynthesis can contribute to the yields of heavy nuclei from intermediate mass AGB stars at low metallicity we have prepared a code which allows all the reactions mentioned above plus neutron captures by numerous heavier nuclides and solves a nuclear kinetics network for the total of 409 particles coupled by 1273 reactions. Neutrons are assumed to have their local equilibrium abundances in every mesh point within the He convective shell.

In all nucleosynthesis codes we used the same input data for the reaction rates. For reactions between charged particles the tables of Caughlan & Fowler (1988, hereafter CF88) were usually used. Exceptions are the reactions ^{17}O(p,α)^{14}N and ^{17}O(p,γ)^{18}F for which the rates proposed by Landré et al. (1990) with the uncertainty factors $f_1 = 0.2$ and $f_2 = 0.1$ recommended by Boothroyd et al. (1995) were preferred, and the reaction ^{12}C$(\alpha,\gamma)^{16}$O whose CF88 rate was multiplied by a constant 1.7 as suggested by Woosley & Weaver (1995). For the NeNa-cycle we also considered the latest nuclear reaction rates advocated by El Eid & Champagne (1995) but did not include them in our main calculations (see Sect. 3). Below, where these new rates for the NeNa-cycle are used instead of those of CF88 we note this explicitly.

Neutron capture cross sections were taken from summaries published by Fowler et al. (1967), Holmes et al. (1976), Woosley et al. (1978), Bao & Käppeler (1987), Ratynski & Käppeler (1988), Beer et al. (1989), Cowan et al. (1991) and Schatz et al. (1995). Beta-decay rates were interpolated in temperature and density using the tables of Takahashi & Yokoi (1987).

Finally, to calculate the structure of a low metallicity massive ZAMS star (Sect. 4) we employed a modified version of Paczyński's code (1970) described by Denissenkov (1990).

Thus, in total, we made use of five different stellar evolution/nucleosynthesis codes in this work.

3. The deep mixing scenario

By the end of the 1970s the fact of star-to-star abundance variations in GCRGs was well established for C and to a lesser extent for N (Bell et al. 1979, Dickens et al. 1979, Norris & Cottrell 1979, Da Costa & Cottrell 1980), while little quantitative information was available for O. In 1979 Sweigart & Mengel found that in low metallicity red giant models the radiative layer where C was transformed into N, and for very low metallicity even the layer where O was transformed into N, were rather well separated from the main part of the HBS where H was transformed into He. This meant that rotationally-driven meridional circulation currents, if present beneath the BCE, could freely penetrate close enough to the HBS and transport outwards material with depleted C and O and enhanced N abundances; usually, a large mean molecular weight gradient forms a barrier which cannot be penetrated by meridional circulation. Further developments of Sweigart & Mengel's idea have been commonly referred to as "the deep mixing (or evolutionary) scenario". It should be noted that in this model the nature of the mixing mechanism is usually not specified. Exceptions are the pioneering work of Sweigart & Mengel (1979) itself and that of Smith & Tout (1992) where meridional circulation in its simplest classical treatment was shown capable of providing the required rate of mixing, and the recent paper of Charbonnel (1995) who considered the more complicated mixing algorithm elaborated by Zahn (1992) which takes into account the interaction between meridional circulation and turbulent diffusion. Other works concentrate on nucleosynthesis aspects of the problem and try to answer the question of whether *any* postulated mixing can explain the whole spectrum of abundance variations (and correlations) seen in globular clusters (as does the present work).

In the 1980s, following the first reports by Cottrell & Da Costa (1981) and Norris et al. (1981) that in NGC 6752 the N enhancements were accompanied by overabundances of Na and Al, evidence accumulated that this was a common feature of many clusters. Moreover, Paltoglou & Norris (1989) found that in ω Cen there is an anticorrelation between Na and O, which anticipated the discovery of the tight global anticorrelation of [O/Fe] versus [Na/Fe] by Kraft et al. (1993). Because it was then absolutely unclear how Na and Al, with rather large nuclear charges (and therefore rather strong Coulomb barriers against charged particle nuclear reactions), could be produced during hydrogen burning in low mass stars, the deep mixing scenario had begun to lose its supporters.

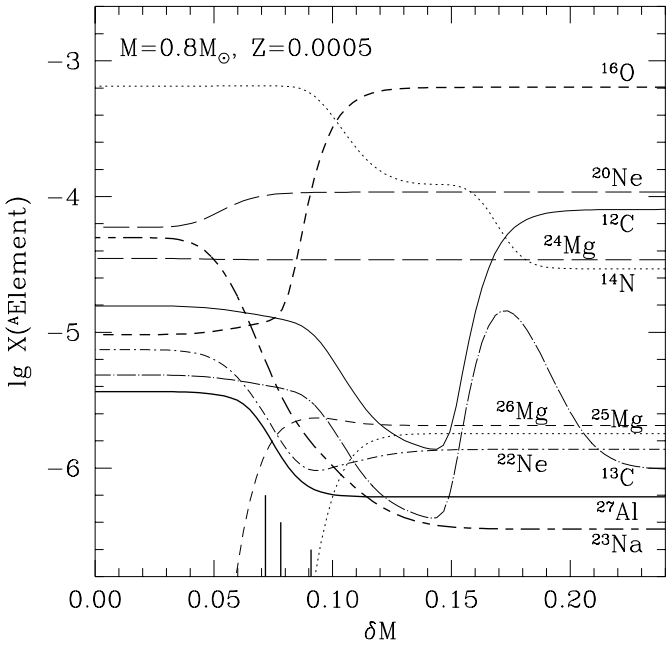

Fig. 1. Abundance profiles for a number of nuclides participating in the CNO-, NeNa- and MgAl-cycles in radiative layers adjacent to the HBS in a $M = 0.8\,M_\odot$ model star having $\lg(L/L_\odot) = 3.0$ and $Z = 5\,10^{-4}$ approximately matching metallicities of the globular clusters M 13 and ω Cen. The mass coordinate δM is measured from the HBS in units of the mass separating the HBS and BCE. The vertical segments on the abscissa show locations of layers where (from right to left) 1, 5 and 10 percent of H were consumed

Its status was rehabilitated by low energy resonances in the reactions ^{22}Ne(p,γ)^{23}Na, ^{25}Mg(p,γ)^{26}Al and ^{26}Mg(p,γ)^{27}Al. First, Denissenkov & Denissenkova (1990) demonstrated that the temperature in the O depleted layer is high enough for the reaction ^{22}Ne(p,γ)^{23}Na to proceed (due to a resonance!) even faster than the reaction ^{16}O(p,γ)^{17}F responsible for the O depletion. Second, Langer et al. (1993) found that ^{27}Al can also be synthesized (mainly at the expense of ^{25}Mg) beneath the O layer in low metallicity red giants. These findings are illustrated in Fig. 1, where abundance profiles for a number of nuclides participating in the CNO-, NeNa- and MgAl-cycles are plotted in the radiative layers adjacent to the HBS in a $M = 0.8\,M_\odot$ model star having $\lg(L/L_\odot) = 3.0$ and $Z = 5\,10^{-4}$. The vertical segments on the abscissa show the locations of layers where (from right to left) 1, 5 and 10 percent of H have been consumed. We will not consider mixing penetrating too deeply into the HBS because: *(i)* on theoretical grounds the molecular weight gradient is expected to stabilize processes inducing both meridional circulation and turbulent diffusion (e.g. Kippenhahn 1974; Talon & Zahn 1997); *(ii)* observed Na abundances constrain the mixing depth (and rate) too (see below); and *(iii)* from the computational point of view, deep mixing is not allowed to bring too much fresh hydrogen fuel into the HBS because otherwise one

would then have to take into account feedback of the mixing on the internal structure and evolution of red giants.

Nucleosynthesis in GCRGs and subsequent mixing have also been discussed recently by Cavallo et al. (1996, 1997) and Langer et al. (1997). The Cavallo et al. papers use detailed stellar interior models to give the physical conditions for the nuclear reactions while that of Langer et al. (1997) does not. They also give useful results for our work and supplement it since they consider effects of different overall metal abundances on the efficiency of deep mixing and also show how nucleosynthesis and mixing in GCRGs self-consistently explain the anomalous abundances of C (as well as the ^{12}C/^{13}C ratios), N, O and Na.

3.1. The initial chemical composition

To calculate the abundance profiles in Fig. 1 we adopted the following initial chemical composition for elements heavier than He: first, all the relevant solar abundances (Anders & Grevesse 1989) were multiplied by a factor $Z/Z_{\odot}$; then the scaled abundances of α-elements (^{16}O, ^{20}Ne, ^{24}Mg and ^{28}Si) were increased by a factor 2.512 to agree with the average value $\langle[\alpha/\mathrm{Fe}]\rangle \approx +0.4$ inferred from field Population II dwarfs (Wheeler et al. 1989); next, abundances of Na and Al were reduced to [Na/Fe] = [Al/Fe] = –0.4 to take into account the even/odd effect (ibid.); and finally, to comply with the global anticorrelation of [O/Fe] versus [Na/Fe] the ^{22}Ne abundance was also decreased to ensure that [^{22}Ne/Na] = 0 (Paper I).

We did not introduce in the initial chemical composition any corrections resulting from the first dredge-up because they were negligible (Sect. 1) compared with the surface abundance changes produced by the following deep mixing. For completeness we note that in our calculations we adopt isotopic ratios ^{24}Mg/^{25}Mg/^{26}Mg = 90/4.5/5.0, except as otherwise stated.

3.2. The CNO and Na abundances

Three further details evident in Fig. 1 are important for the following discussion, and while well-known, are worthy of note. *(i)* As one approaches the HBS the Al abundance increases to a considerably smaller degree than that of Na, with the latter experiencing two successive rises, the first of which appears at the expense of ^{22}Ne while the second is due to consumption of the much more abundant ^{20}Ne. *(ii)* The ^{24}Mg abundance shows no changes at all. It should be emphasized that if one took a pre-core-helium-flash model star one would still find very little ^{24}Mg depletion even well inside the HBS. *(iii)* ^{12}C first decreases with depth and then, after the CN-cycle comes to equilibrium, goes up because in CN-cycle equilibrium the abundance of ^{12}C (and ^{13}C) follow that of N. The latter begins to increase further with depth at the expense of O. Thus the surface abundances of ^{12}C and ^{13}C are expected to behave qualitatively differently from that of, say, O with changing mixing depth (and rate). For example, in a star with *deeper* mixing ($\delta M_{\rm mix} \approx 0.06$) *more* C can survive at the surface than in a star with shallow mixing ($\delta M_{\rm mix} \approx 0.13$).

We have found that deep mixing with the parameters of depth and rate $\delta M_{\rm mix}$= 0.05, $D_{\rm mix}$= $5\,10^8$ cm^2 s^{-1} reproduces quite well all of the observed correlations (or, more precisely, abundance trends) except that of O vs. Al seen in ω Cen, as is shown by the solid lines in Fig. 2. The observational data in the figure have been taken from ND95. We have corrected their N abundances (the average shift applied to [N/Fe] was +0.5 dex) to agree better with the data of Brown & Wallerstein (1993) and Norris & Da Costa (in preparation).

We started our deep mixing calculations with the initial chemical composition described in Sect. 3.1. We do not assume that all low-mass stars in ω Cen (and in any other cluster) had exactly the same abundances before they became red giants because those could be changed by accreting nuclear processed material from a more massive and consequently more evolved companion star in a binary system, for example. Such differences in [C/Fe] among ω Cen giants (see the group of CO-strong stars in Fig. 2) are actually observed. Nevertheless for the present calculations we assume that any range of initial composition is small.

To explain the anticorrelation of O vs. Na in M 13, which is a very good representative of the global anticorrelation of [O/Fe] versus [Na/Fe] in "normal" clusters, we needed to assume a somewhat less deep but faster mixing than in the case of ω Cen: $\delta M_{\rm mix}$= 0.06, $D_{\rm mix}$= $2.5\,10^9$ cm^2 s^{-1}. The reason for these required different mixing rates will not be understood until the deep mixing mechanism itself is understood. This model is shown by the long-dashed lines in Fig. 3 where the observed abundances of Na and Al have been taken from Kraft et al. (1997), and corrected by +0.05 dex and –0.25 dex, respectively, to compensate for differences between the *gf* values adopted in the two works[2]. Note that here, too, there is no agreement between the observed and model results for [Al/Fe] versus [O/Fe]. It is worth commenting that even with the mixing penetrating as deep as $\delta M_{\rm mix} \approx$ 0.05 – 0.06 (cf. Fig. 1), the diffusive mixing rate is such that the amount of additional hydrogen processed in the HBS is relatively small. In the two cases reported here, the final surface H abundances are decreased by only 9.9 and 7.5%, respectively, and Sweigart (1997) has shown that under these circumstances the giant branch evolution is essentially unaltered.

For comparison, the deep mixing solution giving the best fit for the global anticorrelation is also plotted in Fig. 2 (long-dashed lines). From Fig. 2a we infer that ω Cen may contain red giants exhibiting in their atmospheres Na produced not only at the expense of ^{22}Ne but also from ^{20}Ne. That is to say, in some ω Cen stars deep mixing may penetrate even to the second rise of Na seen in Fig. 1. To our knowledge ω Cen is the only example of

[2] These corrections represent the mean differences between the *gf* values of the transitions in common between the two investigations. We note here for the record that we also tested for possible systematic abundances differences which might result from the different formalisms of the Lick group and ND95. We found that when we processed the equivalent widths, *gf* values, and atmospheric parameters of the Lick workers through the ND95 formalism we obtained Na and Al abundances which agreed with theirs to within $\sim$ 0.05 dex.

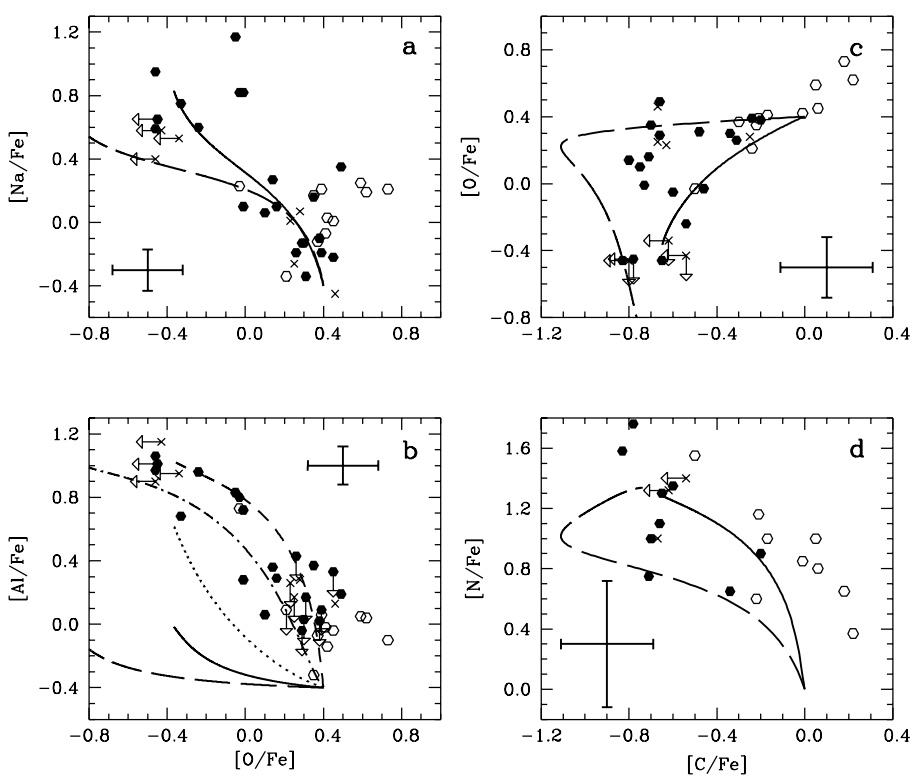

Fig. 2a–d. The abundance trends seen in ω Cen giants (symbols; from ND95) are compared with the results of our deep mixing calculations for two sets of mixing depth and rate ($\delta M_{\rm mix}$; $D_{\rm mix}$, cm^2 s^{-1}): (0.05; $5\,10^8$) – solid, dotted and short-dashed lines, (0.06; $2.5\,10^9$) – long-dashed and dot-short-dashed lines. The former pertains to ω Cen while the latter corresponds to the best fit to the anticorrelation of [O/Fe] versus [Na/Fe] in M 13 (Fig. 3). In panel b the dotted line was calculated with an initial abundance [^{25}Mg/Fe] = 1.2, whereas both the short-dashed and dot-short-dashed lines were determined with [^{25}Mg/Fe] = 1.1 and the ^{26}Al$^{\rm g}$(p,γ)^{27}Si reaction rate increased to 10^3 times the value given by CF88 (see discussion in Sect. 3.4). Open and filled symbols refer to CO-strong and CO-weak stars, and x-es denote stars with unidentified CO status, following ND95. In panel d the N abundances of ND95 have been shifted by +0.5 dex (for them to agree better with the data of Brown & Wallerstein (1993) and Norris & Da Costa (in preparation)). The large crosses indicate observational error bars

globular clusters observed to date where some red giants exhibit in their atmospheres Na produced from both ^{22}Ne and ^{20}Ne, as indicated by our model calculations.

Closer comparison of the results for ω Cen and M 13 shows that the apparent difference between the two clusters is driven by the more metal-rich objects in ω Cen, and we shall return to this point in Sect. 3.5. It suffices here to note that our conclusion on the need for deeper mixing in the ω Cen stars with very strong Na (which also have larger [Fe/H]) will stand, because in more metal-rich objects the regions in which Na is synthesized are closer to the HBS and less accessible for mixing than in the more metal-poor ones (as confirmed by Cavallo et al. 1997).

A detailed analysis of structural and evolutionary differences in the parameters important for the deep mixing scenario between models of red giants having different metallicities has been carried out recently by Cavallo et al. (1997). Their main conclusions concerning the metallicity-dependent effects can be summarized as follows: (*i*) The HBS burns outward in mass quicker with increasing metallicity which allows less time for the nuclear processing of material above the HBS; (*ii*) in the more metal-rich models layers with temperature high enough to alter the envelope abundances lie closer to the HBS, the temperature in these models being lower than in the metal-deficient models. These points have led Cavallo et al. (1997) to the conclusion that "the low-metallicity (evolutionary) sequences should experience greater variations in their surface abundances in more elements than the high-metallicity sequences, assuming mixing does occur". In contradiction to these theoretical expectations the metal-rich giants in ω Cen have larger Na abundances than their metal-poorer counterparts (ND95, for more details see our Sect. 3.5). However, at present this cannot be considered as a serious disagreement between theory and observations because the metal-rich giants in question were selected by ND95 in an extremely biased manner.

A further *unbiased* analysis of abundances in ω Cen giants which are known to show a large range of metallicity is necessary to find observational evidence of the metallicity-dependent effects in deep mixing. Unfortunately, a comparison of abundances in red giants selected from different globular clusters may not be conclusive in this regard because the efficiency of mixing may vary from cluster to cluster.

In ND95 (Sect 5.3.1) the presence of a "floor" to the carbon abundance distribution at [C/Fe]~ -0.8 was suspected. This "floor" finds a natural explanation in the present simulations: sufficiently deep mixing which touches the C rise seen in Fig. 1 (below δM = 0.15) (see comment *(iii)* at the beginning of this section) cannot produce very large surface carbon depletions (compare the solid and the long-dashed lines in Fig. 2c).

The deep mixing calculations for ω Cen giants show that during the last 50% of time spent by the model star between the onset of mixing and the core helium flash the surface ^{12}C/^{13}C ratio declines gradually from 9 to 6, which is in good agreement with values 4–6 reported by Brown & Wallerstein (1989) for objects near the tip of the giant branch.

The dot-long-dashed line in Fig. 3a presents results of our deep mixing calculations performed with the new NeNa-cycle reaction rates (El Eid & Champagne 1995). Its form differs noticeably from that of the long-dashed line calculated with the

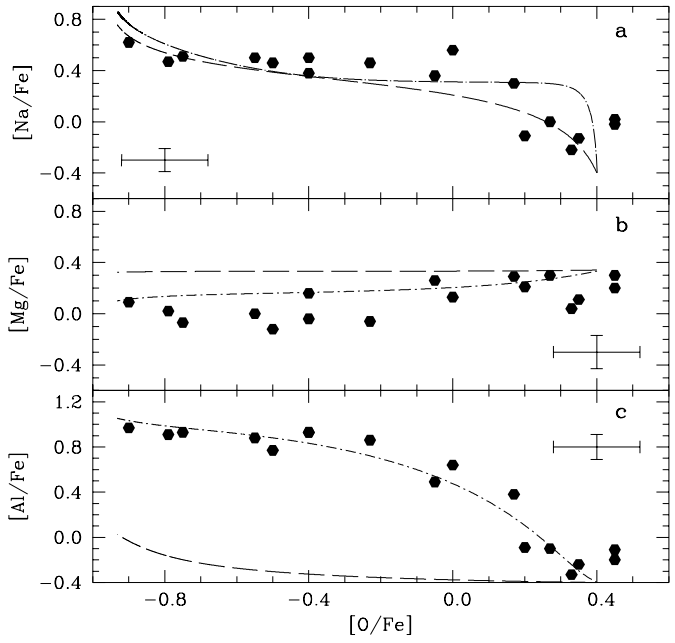

Fig. 3a–c. The anticorrelations of [O/Fe] versus [Na/Fe] and [Al/Fe] and the correlation of [O/Fe] versus [Mg/Fe] seen in M 13 giants (symbols) compared with the results of our deep mixing calculations for $\delta M_{\rm mix}$= 0.06 and $D_{\rm mix}$= 2.5 10^9 cm^2 s^{-1}. Observational data are taken from Kraft et al. (1997) with corrections of +0.05 dex and –0.25 dex applied by us to their [Na/Fe] and [Al/Fe] values, respectively, to compensate for differences between their adopted *gf* values and those of ND95. The dashed lines were computed with standard input physics. The dot-long-dashed line in panel a was calculated with the new NeNa-cycle reaction rates from El Eid & Champagne (1995), while the dot-short-dashed lines (panels **b** and **c**) were calculated with the initial abundances [^{24}Mg/Fe] = 0 (as opposed to the value +0.4 while we normally adopt), [^{25}Mg/Fe] = 1.1 and the ^{26}Al$^{\rm g}$(p,γ)^{27}Si reaction rate increased to 10^3 times the CF88 value. The large crosses indicate observational error bars

CF88 reaction rates, especially in the range $0 \leq$[O/Fe]≤ 0.4. This difference is entirely due to the considerably higher new rate of the reaction ^{22}Ne(p,γ)^{23}Na which causes a shift of the first rise of the Na abundance far outwards from the O depleted layer (Fig. 4). As a result, deep mixing first quickly produces a large Na enrichment at the stellar surface and only then does the surface O abundance begin to decline. Unfortunately, observational errors in the spectroscopic abundance analysis do not allow us to make a definitive choice between the old and new reaction rates from inspection of Fig. 3a.

To summarize, the deep mixing scenario can explain evolutionary changes in the abundances of C (and ^{12}C/^{13}C ratios), N, O and Na. It fails, however, to interpret the anticorrelation of [O/Fe] vs. [Al/Fe] (Fig. 2b, solid line and Fig. 3c, long-dashed line) and the correlation of [O/Fe] vs. [Mg/Fe] (Fig. 3b, long-dashed line).

3.3. When does the deep mixing start?

In the above considerations of both M 13 and ω Cen we started our deep mixing calculations with a model star in which the HBS had just crossed the H-He discontinuity left behind by the BCE at the end of the first dredge-up. This and several neighbouring models are characterized by a small drop in luminosity caused by the adjustment of the HBS to an increased fuel supply when it encounters the H-He discontinuity. Stellar evolution slows down near this point and as a result a (subgiant) bump in the globular-cluster luminosity function appears at the corresponding visual magnitude. It was Sweigart & Mengel (1979) who proposed that deep mixing started only with that model because in preceding models there was a molecular weight gradient between the HBS and the BCE built up during the MS hydrogen burning which did not permit mixing (meridional circulation) to operate. Observations of anomalous evolutionary changes of ^{12}C/^{13}C and of the ^{3}He and ^{7}Li abundances in evolved halo stars seem to support this idea (Charbonnel 1995). It is, however, clearly at odds with the observations in clusters such as M92 which show depletions of carbon well below the level postulated by Sweigart & Mengel (Langer et al. 1986). Moreover, recent spectroscopic analysis of red giants in M 13 (Kraft et al. 1997) has revealed stars with enhanced Na and Al and depleted O (and even Mg!) at luminosities low enough to draw the conclusion that at least in the giants of M 13 deep mixing (if it is responsible for the observed abundance variations) begins earlier than Sweigart & Mengel thought. Our comment on this point is as follows. Inspection of the chemical structure of our models shows that the molecular weight gradient built up during the MS hydrogen burning is *by far less steep* than the gradient at the point of deepest penetration of the postulated deep mixing which has to be overcome in order to dredge up freshly synthesized Al and even Na (if the reaction rates of CF88 are used). We therefore infer that in every globular cluster having red giants with enhanced Al (and Na) and depleted O, even though we cannot identify the process responsible, deep mixing began to operate well before the point suggested by Sweigart & Mengel.

A potential serious problem for deep mixing could be overcoming the H-He discontinuity where, in canonical evolution, the mean molecular weight experiences a jump within a very narrow mass interval as a result of the deepest penetration of the convective envelope. Since mixing signatures, such as C-depletions, are seen at luminosities well below that at which the HBS reaches this composition discontinuity (e.g. M92, Langer et al. 1986), we must postulate that the mixing processes, perhaps acting in concert with variable convective overshoot, prevent this discontinuity from arising (or smooth it out). On the other hand, the luminosity function bump that is predicted when the HBS burns through this discontinuity, is observed in many globular clusters (e.g. Alongi et al. 1991). Consequently, in these clusters, not all of the evolving red giants can have had the discontinuity smoothed away.

3.4. The Mg and Al abundances

As may be seen in Fig. 1, aluminium cannot be produced at the expense of ^{24}Mg in standard evolutionary calculations (see also comment *(ii)* on Fig. 1 at the beginning of Sect. 3.2). On the other hand, ^{25}Mg does make Al (Fig. 1) but in amounts

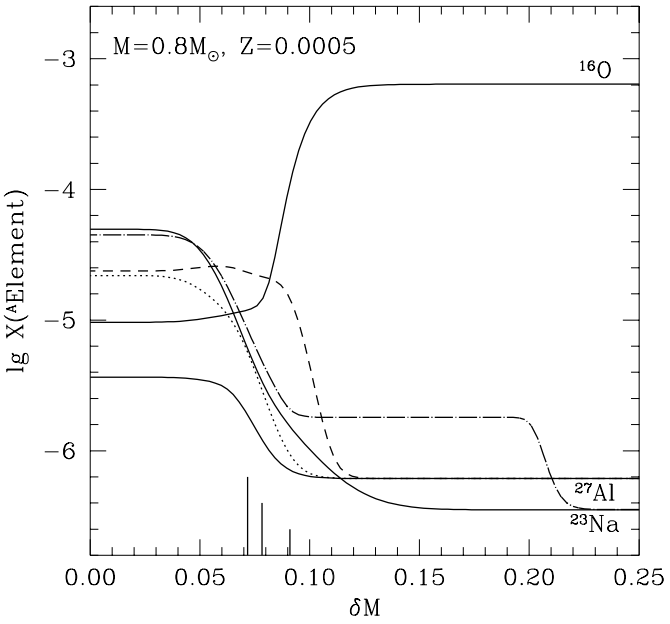

Fig. 4. Na and Al abundance distributions close to the HBS, calculated under different assumptions: standard assumptions (see text) – solid lines; new NeNa-cycle reaction rates from El Eid & Champagne (1995) – dot-long-dashed line; initial abundance [^{25}Mg/Fe] = 1.2 – dotted line; [^{25}Mg/Fe] = 1.1 and the ^{26}Al^g(p,γ)^{27}Si reaction rate from CF88 multiplied by the factor 10^3 – short-dashed line

which are too small to explain the observations in ω Cen (see Fig. 2b, solid line) and M 13 (Fig. 3c, long-dashed line). Until recently one could speculate that in (some) GCRGs the initial ^{25}Mg abundance might be anomalously large as compared to its scaled solar value (e.g. Langer & Hoffman 1995; Paper I). In the solar chemical composition ^{24}Mg is the most abundant magnesium isotope: ^{24}Mg/^{25}Mg/^{26}Mg = 79/10/11 (Anders & Grevesse 1989). If one assumes that [^{25}Mg/Fe]> 1.0, then one can produce the observed Al enhancements of about +1 dex (see below). Due, however, to an increased contribution of ^{25}Mg to the sum Mg = ^{24}Mg+^{25}Mg+^{26}Mg and the evolutionary transformation of this ^{25}Mg into Al one would then expect the total magnesium abundance [Mg/Fe] to decline with increasing [Al/Fe]. Recently such an observational trend has been found in M 13 giants (Fig. 3b, symbols) by Shetrone (1996a) and Kraft et al. (1997). On the other hand, analysis of isotopic magnesium composition in a sample of 6 stars in M 13 (S96; Shetrone 1997) unexpectedly demonstrated that stars with extremely large [Al/Fe] possessed noticeably reduced ^{24}Mg and not ^{25}Mg ($\langle$[^{24}Mg/Fe]$\rangle = -0.33$ for 5 stars with the largest [Al/Fe]). It should be noted that the same analysis revealed (for the first time in any star ever observed!) anomalous magnesium isotopic ratios with an unusually increased contribution of the sum ^{25}Mg+^{26}Mg ([^{25}Mg+^{26}Mg/Fe] up to +0.21, average fractions of the magnesium isotopes $\langle^{24}$Mg$\rangle/\langle^{25}$Mg$\rangle/\langle^{26}$Mg$\rangle$ = 56/22/22). Unfortunately, S96's analysis was not able to separate the ^{25}Mg and ^{26}Mg isotopes and gave only their summed abundance, and consequently, in deriving the magnesium isotopic ratios ^{25}Mg and ^{26}Mg were assumed to have identical abundances.

A straightforward interpretation of the anticorrelation of [Mg/Fe] versus [Al/Fe] in the M 13 giants, which guarantees an explanation of the O vs. Al anticorrelations in the clusters M 13 and ω Cen and which also takes into account the results of S96's isotopic analysis is to suppose that there is a strong but still undetected low energy resonance in the reaction ^{24}Mg(p,γ)^{25}Al. Unfortunately, at present we cannot estimate the strength of the resonance because we do not know its energy which also strongly influences the reaction rate. However, we note that the resonance has to provide this reaction with a rate comparable with that of the ^{25}Mg(p,γ)^{26}Al one in order to ensure that the deep mixing reaches the depth where ^{24}Mg is depleted (see the ^{25}Mg profile in Fig. 1). In this case aluminium would be a product of the chain of reactions ^{24}Mg(p,γ)^{25}Al($\beta^+\nu$)^{25}Mg(p,γ)^{26}Al^g(p,γ)^{27}Si($\beta^+\nu$)^{27}Al and the beta-decay ^{26}Al^g($\beta^+\nu$)^{26}Mg together with the channel ^{25}Mg(p,γ)^{26}Al^m($\beta^+\nu$)^{26}Mg would take care of a large final abundance of the sum ^{25}Mg+^{26}Mg then dominated by ^{26}Mg. "Unfortunately", nuclear physicists seem to have little (if any) doubt concerning the current ^{24}Mg(p,γ)^{25}Al reaction rate (Arnould et al. 1995; Zaidins & Langer 1997). Nevertheless, it would be interesting to know whether they can *guarantee* that such a low energy resonance does not exist. Of course, any further experimental studies of the MgAl-cycle reaction rates would be well worthwhile.

It should be noted that uncertainties in the NeNa cycle reactions rates also affect the overall Mg abundances because of leakage from the NeNa cycle into ^{24}Mg, the rates advocated by El Eid & Champagne (1995) giving more efficient leakage than the rates of CF88. However, as a result of using the El Eid & Champagne NeNa cycle rates it becomes even more difficult to reduce the ^{24}Mg abundance in the HBS (Cavallo et al. 1997) which in turn makes it more difficult to explain the MgAl anticorrelation in the deep mixing scenario.

An alternative is that in GCRGs with enhanced Na and Al and depleted O and Mg abundances we actually observe products of hydrogen burning which has occurred at much higher temperatures (say, at $T_6 \equiv T/10^6\,\mathrm{K} \sim 70$) than those reached in the HBS in the standard stellar models ($T_6 \leq 55$). We will explore this possibility in the next section.

In the event that the above two suggestions cannot be realized, a third and final possibility is to postulate that the extremely large Al enhancements in GCRGs are a signature of an unusually overabundant initial ^{25}Mg. But now, to comply with the results of S96's magnesium isotopic analysis, we have also to explain how stars with especially large initial ^{25}Mg abundances acquired a deficit in ^{24}Mg. In Sect. 4 we will consider a primordial source which is able (in principle) to produce such an abundance mixture and until then we merely assume that low mass stars in M 13 and ω Cen had initially increased ^{25}Mg.

The dotted line in Fig. 2b (see also Fig. 4) shows how [Al/Fe] evolves with [O/Fe] in ω Cen giants in the case of an initial abundance [^{25}Mg/Fe] = 1.2. Here we used the same values of $\delta M_{\rm mix}$ and $D_{\rm mix}$ as earlier because they had given good fits to the

other three abundance trends seen in ω Cen. Unfortunately, the new calculations disagree with observations both quantitatively (there is not enough Al produced) and qualitatively (the dotted line has a slope different from that hinted at by the observations). The quantitative disagreement is caused by the fact that with CF88 reaction rates the channel ^{25}Mg(p,γ)^{26}Al($\beta^+\nu$)^{26}Mg dominates over the ^{27}Al producing channel (see above), and as a result, a large fraction of ^{25}Mg is wasted to synthesize ^{26}Mg instead of ^{27}Al. The wrong slope of the theoretical dependence of [Al/Fe] on [O/Fe] comes from the necessity of waiting until a large enough abundance of ^{26}Al$^{\rm g}$ is built up for the chain of reactions ^{26}Al$^{\rm g}$(p,γ)^{27}Si($\beta^+\nu$)^{27}Al to begin competing with the beta-decay ^{26}Al$^{\rm g}$($\beta^+\nu$)^{26}Mg. These undesirable effects can be diminished by choosing a faster ^{26}Al$^{\rm g}$(p,γ)^{27}Si reaction rate. Indeed, according to Arnould et al. (1995), for the range of temperatures found in the HBS in GCRGs ($T_6 \sim 40 - 50$) the ^{26}Al$^{\rm g}$(p,γ)^{27}Si reaction rate may be underestimated by a large factor of $\sim 10^3$ in CF88. If this acceleration factor is applied, the ^{27}Al producing channel gets so wide that now one can even use a somewhat smaller value of the initial ^{25}Mg abundance. In Fig. 2b (see also Fig. 4) the short-dashed line was calculated with [^{25}Mg/Fe] = 1.1 and the ^{26}Al$^{\rm g}$(p,γ)^{27}Si reaction rate equal to 10^3 times its CF88 value. The dot-short-dashed lines in Figs. 2b and 3c were calculated under the same assumptions but for the mixing depth and rate required by the O vs. Na anticorrelation in M 13. Now theory matches the observations! The initial ^{24}Mg abundance has no influence on the results of these calculations. In Fig. 3b the dot-short-dashed line is obtained assuming the initial abundance [^{24}Mg/Fe] = 0 (instead of +0.4) which, as expected, produces a decline of the total magnesium abundance [Mg/Fe] with increasing [Al/Fe] due to consumption of the now abundant ^{25}Mg. It seems, however, that observations demand even a larger (initial) deficit in ^{24}Mg.

The adoption of [^{24}Mg/Fe] = 0, [^{25}Mg/Fe] = 1.1 and [^{26}Mg/Fe] = 0 results in [^{25}Mg+^{26}Mg/Fe] = 0.81, [Mg/Fe] = 0.33 and ^{24}Mg/^{25}Mg/^{26}Mg = 37/58/5, i.e. a ^{25}Mg dominated mixture of the magnesium isotopes; and for the deep mixing presumably operating in M 13 giants ($\delta M_{\rm mix} = 0.06$, $D_{\rm mix} = 2.5\,10^9$ cm^2 s^{-1}) just before the core helium flash we find [^{24}Mg/Fe] = 0.004, [^{25}Mg/Fe] = –0.86, [^{26}Mg/Fe] = 0.61 and, consequently, [^{25}Mg+^{26}Mg/Fe] = 0.35, [Mg/Fe] = 0.10 and ^{24}Mg/^{25}Mg/^{26}Mg = 64/1/35. Since, however, the observations *cannot separate* ^{25}Mg and ^{26}Mg this final mixture is not distinguished from the one ^{24}Mg/^{25}Mg/^{26}Mg = 64/18/18 which has the ratios close to the average ones reported by S96.

Shetrone interpreted his results of the magnesium isotopic analysis in terms of the ^{25}Mg and ^{26}Mg abundances remaining unchanged during deep mixing. But as we have seen there are two alternative interpretations: *(i)* initially the magnesium isotope mixture consisted of almost pure ^{24}Mg (as, for instance, in the M 13 giant L598 of S96's sample which has ^{24}Mg/^{25}Mg/^{26}Mg = 94/3/3, and which shows little evidence of mixing); if, in addition, there is a strong low energy resonance in the reaction ^{24}Mg(p,γ)^{25}Al, then after mixing we will have ^{24}Mg depleted and both the sum ^{25}Mg+^{26}Mg and ^{27}Al, enhanced; *(ii)* initially ^{24}Mg was depleted and ^{25}Mg substantially increased (primordially!); during deep mixing the ^{24}Mg abundance remains constant and that of ^{27}Al increases at the expense of ^{25}Mg, the sum ^{25}Mg+^{26}Mg being dominated by ^{26}Mg which is also produced from ^{25}Mg. In both cases one obtains approximately what Shetrone has observed.

3.5. Metallicity dependent effects in ω Cen

We noted in Sect. 3.2 that the more metal-rich stars in ω Cen were in large part responsible for the apparent differences between it and M 13. In Fig. 5 we divide the ω Cen sample into two abundance groups: on the left are objects having [Fe/H] $<$ –1.3, and in the middle those with [Fe/H] $>$ –1.3. On the right, for comparison purposes, we also show data for the metal-richer globular clusters M5 ([Fe/H] = –1.2) and M71 ([Fe/H] = –0.8) from Shetrone (1996a). To focus further discussion we also superimpose on the diagrams the model fits for Na in M 13 (the dashed line from Fig. 3a).

Inspection of the figure reveals several interesting points. First, concerning Na, one sees that the metal-poorer objects in ω Cen have an [Na/Fe] versus [O/Fe] correlation similar to that seen in M 13. In contrast, however, the metal-rich ω Cen stars have [Na/Fe] values which are larger by $\sim$ 0.4 dex than in M 13. Such large Na enhancements do not exist in the M5 and M71 sample, which has comparable [Fe/H].

Second, concerning Mg, we see among the metal-poor ω Cen group the same [Mg/Fe] versus [O/Fe] correlation as discussed by Shetrone (1996a) and Kraft et al. (1997) for M13. The spread in [Mg/Fe] ($\sim$ 0.5–0.6), appears to be slightly larger that observed for M 13 in Fig. 3 ($\sim$ 0.3), suggestive of more extreme mixing in ω Cen. This is, however, very different from the behaviour of [Mg/Fe] versus [O/Fe] in the metal-rich ω Cen stars, where one sees little evidence for a spread in [Mg/Fe].

Finally, both groups of ω Cen stars appear to exhibit the same [Al/Fe] versus [O/Fe] behavior. A concomitant, important, point is that there is little if any dependence of [Mg/Fe] on [Al/Fe] in the metal-rich ω Cen giants, in stark contrast to what is found in the metal-poor ω Cen and M 13 giants!

One may summarize the above results by stating that the mixed metal-rich giants in ω Cen, in comparison with their metal-poorer counterparts, have similar Al enhancements, larger Na enhancements, and no accompanying Mg depletion. The metal-rich ω Cen stars clearly offer an important constraint on our understanding of the manner in which they have been enriched. For those who would take up the challenge we provide the following information and caveats. The mixed objects in question are ROA 150, 162, 231, 248, 357, 371 and 480, and were included in the work of ND95 in an extremely biased manner as examples of objects having the most extreme abundance peculiarites in the cluster. All have enhancements of the s-process elements, which ND95 attribute to primordial enhancement from low mass AGB stars. They have no counterpart in the more metal-rich clusters, such as M5 and M71.

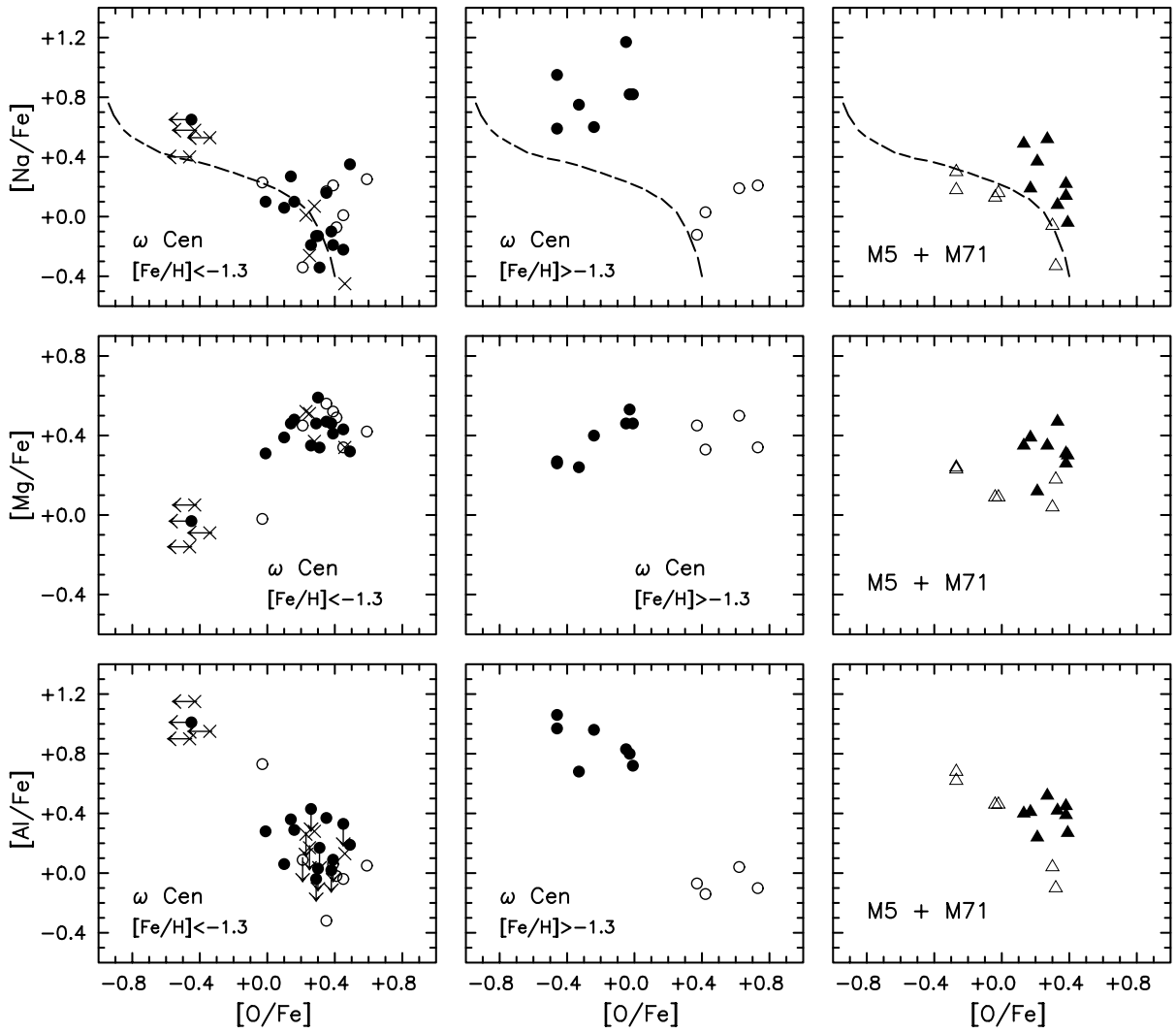

Fig. 5. The dependence of [Na/Fe], [Mg/Fe] and [Al/Fe] on [Fe/H] for (left) ω Cen giants with [Fe/H] $<$ –1.3, (middle) ω Cen stars with [Fe/H] $>$ –1.3, and (right) M5 and M71 giants. For ω Cen the symbols are as defined in Fig. 2, while for M5 (open triangles) and M71 (filled triangles) the data have been taken from Shetrone (1996a) corrected by +0.05 and –0.25 for Na and Al as in Fig. 3. The dashed lines are the deep mixing simulation for Na in M 13 shown in Fig. 3a

4. The primordial scenario

In the primordial scenario, star-to-star abundance variations in globular clusters are thought to be produced before or during formation of low mass stars. Possible sources of primordial pollution include winds from massive stars, SNe explosions, winds and planetary nebulae (PNe) ejection by AGB stars and novae. Are any traces of nucleosynthesis yields from the earlier generations of stars seen in globular clusters? If one assumes that protoglobular clusters formed from material having the big bang chemical composition with zero heavy element content, then the answer is definitely yes, since in present-day clusters stars show a wide spectrum of elements heavier than helium, and one is forced to seek such primordial sources.

The first objects to contribute to the self-enrichment of globular clusters are massive stars during hydrostatic mass loss and on their final evolutionary stage – SNeII (we do not consider the hypothesized Very Massive Objects). The modern radiation-driven wind theory (Kudritzki et al. 1991; Jura 1986) predicts, however, that during hydrostatic evolution massive stars with Z = 0 will not lose a considerable amount of their mass (Maeder 1992). Therefore, the only nucleosynthesis yields from the first generation of massive stars are most probably those produced by SNeII and consist mainly of O (and other α-elements) (Woosley & Weaver 1995). It is also important to note that as argued by Laird & Sneden (1996) and Carney (1996) there is no evidence for any *progressive enrichment* of clusters by the SNeIa responsible for the production of the iron-peak elements in Galactic chemical evolution (Timmes et al. 1995, hereafter TWW95) and which chronologically follow SNeII.

The next potential polluters of the intracluster medium are AGB stars. ND95 reported that abundances of the heavy neutron-addition elements, which are presumably produced in the s-process nucleosynthesis in $1-3\,M_{\odot}$ AGB stars rise as

[Fe/H] increases in ω Cen red giants. Since intermediate mass stars ($3 - 8\,M_\odot$) evolve faster than $1 - 3\,M_\odot$ objects, one expects that some products of nucleosynthesis from intermediate mass AGB stars could also be present in the material captured by contracting low mass stars in globular clusters or accreted by them later.

4.1. Nucleosynthesis yields from SNe

The chemical enrichment history of globular clusters seems to be quite different from the chemical evolution of the bulk of the Galaxy. One of the plausible scenarios of globular cluster formation was proposed by Cayrel (1986) and elaborated upon further by Brown et al. (1991b, 1995). In this scenario massive stars form first in a protocluster's dense core from material having the big bang composition. They evolve rather quickly (on a time scale of $\sim 10^6 - 10^7$ years) and explode as SNeII without leaving any remnants. A supershell produced by shocks from the multiple SNe explosions sweeps up and compresses the protocluster material which now consists of a mixture of the big bang and SNeII ejecta compositions. It is this supershell that becomes the birthplace for stars covering the whole mass spectrum. There are a number of arguments, both theoretical and observational, supporting this scenario (see the papers cited above). One of these is the absence of low mass stars having the primordial big bang composition. We shall not, however, discuss here all advantages and disadvantages of different globular clusters formation models. We merely emphasize that both intermediate and low mass stars in globulars were very likely to form out of material polluted by SNeII. Two things are necessary to specify the element abundances in this material: first, mass dependent nucleosynthesis yields from the SNeII whose progenitors had the big bang initial composition, and second, an estimate of dilution of these yields in the supershell.

In Fig. 6 the abundances of some of the SNeII ejecta which are important for our work are presented as functions of the initial mass of the SN progenitor (which is also its final mass because in these calculations stellar winds were not taken into account) for $Z = 0$ for the models of Woosley & Weaver (1995) as adopted by TWW95 (their Sect. 2.4). One should bear that in mind, however, that the ejecta composition of SN models is more uncertain at higher masses; for example, the Na/O production of the 30 $M_\odot$ models varies by almost a factor of 500 (Woosley & Weaver 1995). The large variations of abundances from star to star are mainly caused by the uncertainty in modelling the explosion and the sensitivity of models to the interaction between various convective zones during the late stages of the evolution. Despite these large random-like abundance variations TWW95 argue that after convolution with an appropriate initial mass function and integrating over time one gets quite reasonable results, and indeed they do succeed in reproducing the observed evolutionary changes of abundances for a large number of elements lighter than zinc in a simple model of galactic chemical evolution.

The range of masses of the SN progenitors in Fig. 6 is $12 \le M/M_\odot \le 40$. Following TWW95 and Cayrel (1986) we

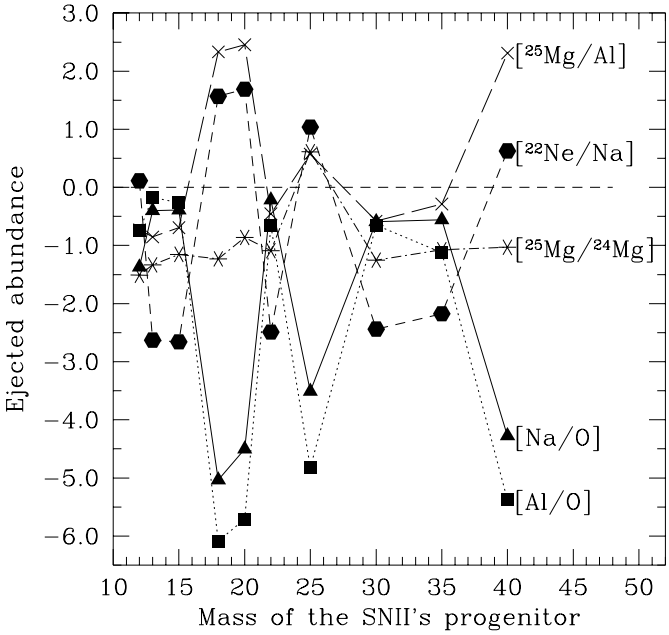

Fig. 6. Abundances of some nuclides ejected by SNeII (following Woosley & Weaver 1995)

assume that the initial mass function in the protoglobular cluster's dense core was a low mass cutoff Salpeter (1955) power law $\Psi(M) \propto M^{-(1+x)}$ with a slightly different exponent of $x = 1.31$ (instead of 1.35) which gave the best fit to the observed element evolution. After convolution of the abundances from Fig. 6 with $\Psi(M)$ over the range 12 – 40 $M_\odot$ we find the average abundances ejected by SNeII. The latter are diluted in the supershell by material having the big bang composition. The dilution coefficient can be estimated as the ratio $v_s/v_{ej} \sim 10^{-3}$ of the local intracluster sound velocity $v_s \sim 10\,\mathrm{km\,s^{-1}}$ to the initial velocity of the SN's ejecta $v_{ej} \sim 10^4\,\mathrm{km\,s^{-1}}$ (Cayrel 1986). This estimate neglects the adiabatic phase of the SN's expansion and takes into account only the "snowplow" phase. In Table 1 the final abundances expected as a result of SNeII explosions and subsequent dilution in the supershell are presented.

From these data we draw the following conclusions: *(i)* the value of [Fe/H] corresponds to that of the most metal-deficient globular clusters; *(ii)* the values of [α/Fe] are lower than observed in globular clusters which results, in large part, from the overproducton of Fe in the model supernovae (see TWW95); *(iii)* N is extremely underabundant; *(iv)* the ^{22}Ne/Na ratio is far less than the initial one assumed in GCRGs (Sect. 3.1); *(v)* abundances of ^{25}Mg and ^{26}Mg are very low compared to ^{24}Mg and Al. Inspection of Fig. 6 shows that the conclusion concerning the very low ^{25}Mg/^{24}Mg ratio in the primordial mixture is rather robust. We thus have to look for other nucleosynthesis source(s) of ^{22}Ne, ^{25}Mg and ^{26}Mg. TWW95 proposed the intermediate mass AGB stars as the main producers of the ^{25}Mg and ^{26}Mg isotopes. Our calculations support this idea (see below). As regards N, TWW95 reported that its abundance in SNeII ejecta can be much larger if one takes into account some convective

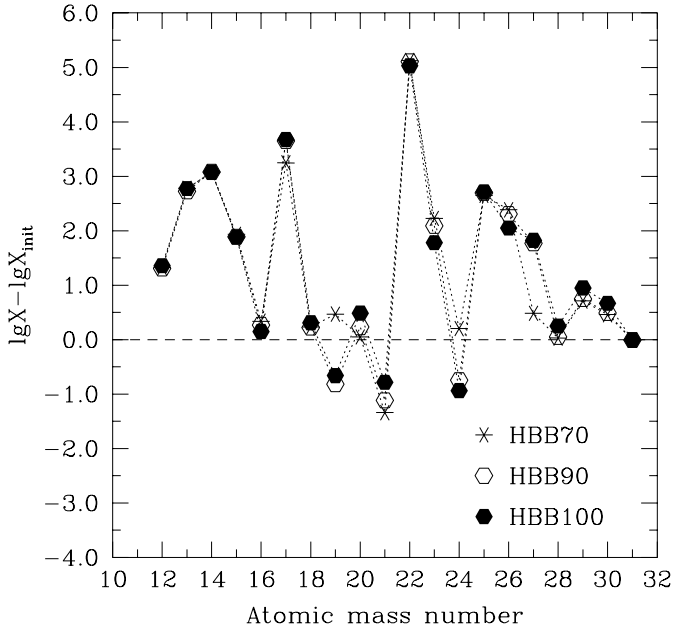

Fig. 7. Nucleosynthesis yields of some light nuclides from intermediate mass AGB stars after 400 pulses. The notation HBBT6 signifies that HBB was assumed to occur at the temperature T6 10^6 K. The atomic mass number 26 corresponds to ^{26}Mg. The initial chemical composition was that given in Table 1

Table 1. Abundances expected as the result of SNeII explosions

abundance(s)	SNeII
[C/Fe]	–0.25
[N/Fe]	–2.44
[O/Fe]	–0.05
[^{20}Ne/Fe]	+0.10
[Na/Fe]	–0.52
[^{24}Mg/Fe]	–0.05
[^{25}Mg/Fe]	–1.25
[^{26}Mg/Fe]	–1.27
[Mg/Fe]	–0.15
[Al/Fe]	–0.67
[Si/Fe]	–0.15
[Fe/H]	–2.31
[^{22}Ne/Na]	–2.34
[^{25}Mg+^{26}Mg/Al]	–0.59
^{24}Mg/^{25}Mg/^{26}Mg	98/1/1

overshoot in the low metallicity SNII's progenitor but they also infer that AGB stars can contribute much to the galactic N (and C) production.

4.2. Yields from intermediate mass AGB stars

To take into account the contribution to galactic chemical evolution from intermediate mass AGB stars TWW95 made use of the results of parameterized nucleosynthesis calculations by Renzini & Voli (1981) who, however, followed only the evolution of abundances of ^{12}C, ^{13}C, ^{14}N and ^{16}O for $Z \geq 0.004$. Our calculations supplement those of Renzini & Voli in two respects. First, we consider also the evolution of elements heavier than O and, second, we choose Z as low as 10^{-4} and allow different relative distributions of nuclides within Z which turns out to have a pronounced effect on the final abundances.

As a representative of intermediate mass AGB stars we considered a $5\,M_\odot$ object. Thermal pulses of the helium burning shell started with the core mass $M_{\rm c} = 0.96\,M_\odot$. It should be emphasized again that we did not follow the AGB stellar evolution. Instead we considered the parameterized nucleosynthesis in the $5\,M_\odot$ AGB star following the description of Renzini & Voli (1981) (for more details see Paper II). The core mass is constrained to remain smaller than the Chandrasekhar limit $M_{\rm Ch} \sim 1.4\,M_\odot$, but long before $M_{\rm c}$ could approach $M_{\rm Ch}$ some kind of instability is believed to force envelope ejection in the form of a PN which terminates AGB evolution (Renzini 1981; Wagenhuber & Weiss 1994). The exact upper limit for the number of pulses before the PN's ejection is not known. It can be approximately constrained by the observed relation between white dwarf masses and the initial masses of their MS progenitors. Such relations show that intermediate mass stars with lower metallicity may survive longer on the AGB (Weidemann 1987). We have chosen $N = 400$ as the limiting number of pulses in our low metallicity AGB nucleosynthesis calculations. This number results in the final core mass $M_{\rm c} = 1.12\,M_\odot$. We are aware that the chosen value of N may be overestimated, but smaller values ($N = 100 - 200$) give the same qualitative (but of course less pronounced quantitative) results. The initial chemical composition is that given in Table 1.

In Fig. 7 the final (i.e. after 400 pulses) surface abundances in the envelope of the $5\,M_\odot$ AGB star are plotted for three different hot bottom burning (HBB) temperatures: $T_{\rm HBB} = 70, 90$ and $100\,10^6$ K. It should be noted that the model value of $T_{\rm HBB}$ is also very uncertain because it strongly depends on the depth within the HBS which can be reached by the BCE during the interpulse period, with the depth being very sensitive to the poorly known extent of convective overshoot (Lattanzio & Frost 1997). Unfortunately, it is $T_{\rm HBB}$ that determines whether ^{24}Mg is transformed into Al at the BCE (Fig. 7). The initial chemical composition for these calculations was that given in Table 1 (see Sect. 4.1).

From Fig. 7 we infer that if HBB is neglected (this approximately corresponds to the results shown by asterisks for $T_{\rm HBB} = 70\,10^6$ K) the main new results (as compared to those obtained by Renzini & Voli (1981)) are considerable increases of the ^{22}Ne/Na ratio and of the ^{25}Mg and ^{26}Mg abundances. The ^{22}Ne, ^{25}Mg and ^{26}Mg isotopes are primarily produced by α-capture reactions whereas Na is synthesized in the reactions ^{22}Ne(n,γ)^{23}Ne($\beta^-\overline{\nu}$)^{23}Na. Aluminium is not produced during pulses because there are no α-capture reactions which result in Al, on the one hand, and the neutron capture cross section for the reaction ^{26}Mg(n,γ)^{27}Mg followed by the beta-decay ^{27}Mg($\beta^-\overline{\nu}$)^{27}Al is very low ($\sigma_{\rm n\gamma} = 0.084$ mb), on the other.

In Table 2 we compare the abundances of ^{22}Ne, Na, ^{25}Mg and ^{26}Mg which are achieved in the H-He intershell just af-

Table 2. Abundances ($\lg X/X_{\rm i}$) in the H-He intershell of the $5\,M_\odot$ AGB star after the 400th pulse

chem. comp.	^{22}Ne	Na	^{25}Mg	^{26}Mg
solar	2.06	1.57	1.40	1.05
$Z = 0.0001^a$	2.36	2.19	1.69	1.20
SNeII^b	4.80	1.79	2.51	1.98

(a) the relative distribution of heavy nuclides within Z is described in Sect. 3.1; (b) the initial composition from Table 1.

ter the 400th pulse for three initial compositions: (1) solar; (2) $Z = 10^{-4}$ and the relative abundance distribution as described in Sect. 3.1; (3) abundances from Table 1. We see that especially large increases of the ratio ^{22}Ne/Na and of the ^{25}Mg and ^{26}Mg abundances are obtained for the third mixture, which was derived from the globular cluster self-enrichment model.

In Paper II our estimate of the fraction of material which first takes part in the nucleosynthesis processes in intermediate mass AGB stars and is later captured by low mass stars q (the dilution coefficient) was $0.1 - 0.2$. This estimate assumes homogeneous distribution of the processed material among low mass stars. While this assumption appears to be good one for the nucleosynthesis yields from SNe because the post-shock turbulence is thought to mix the protocluster material well (Brown et al. 1995), yields from AGB stars are most likely to be distributed inhomogeneously and primarily captured by low mass stars nearest to them during ejection of their envelopes. In this case the coefficient q may be even larger.

The discussion given above supports the idea that intermediate mass AGB stars could be a source of the increased initial ^{25}Mg (and ^{26}Mg) abundance in GCRGs. Indeed, it follows from Fig. 7 that a value of $q \geq 0.2$ would be quite enough to increase the ^{25}Mg abundance from [^{25}Mg/Fe] = –0.59 (Table 1) up to [^{25}Mg/Fe]$\geq$ 1.0 as required by our deep mixing calculations (Sect. 3.4). At the same time this would bring the ^{22}Ne/Na ratio close to the value [^{22}Ne/Na] = 0 which makes possible the synthesis of Na in GCRGs inferred to occur at the expense of ^{22}Ne.

Our calculations of the nucleosynthesis yields from the $5\,M_\odot$ AGB star confirm the conclusion of TWW95 that AGB stars can contribute to the enrichment of the interstellar medium (and in our case of low mass stars in globular clusters) in C and N. We also repeat our result from Paper II that the intermediate mass AGB stars can be responsible for some primordial enrichment of low mass stars in Na and Al (Fig. 7). Contrary, however, to the situation for Na, which is produced during pulses, Al is produced from ^{24}Mg only during HBB, the details of which are not fully constrained by theory. At temperatures higher than about 70 10^6 K the ^{24}Mg(p,γ)^{25}Al reaction goes faster than proton captures by ^{25}Mg and ^{26}Mg (CF88), the latter two isotopes being also produced copiously during pulses. As a result of very hot bottom burning ($T_{\rm HBB} \geq 90\,10^6$ K) which is predicted by recent evolutionary calculations (Lattanzio et al. 1997), the ^{25}Mg enhancement can be accompanied by a deficit of ^{24}Mg and by an increase of Al. In order, however, to produce low mass stars with even a twofold decrease of the initial ^{24}Mg abundance we need a dilution coefficient as large as $q = 0.5$ and of course in addition we get some primordial Al enhancement. It should be noted that the abundance of O is not reduced as the result of HBB in intermediate mass AGB stars (Fig. 7) since O is synthesized from C during pulses. Deep mixing in red giants is therefore still required.

To summarize, the advantages of the proposed primordial scenario are the following: *(i)* it supplies low mass stars with a large initial abundance of ^{25}Mg; *(ii)* it explains why in GCRGs with especially large Al enhancements some ^{24}Mg depletion is also observed (because low mass stars with a low initial ^{24}Mg abundance are expected to possess a large initial ^{25}Mg); *(iii)* it accounts for some C (and N) primordial enrichment of low mass stars as is observed in globular clusters (Fig. 2, open symbols). Its apparent deficiencies are: *(i)* it assumes rather large dilution coefficients ($q \geq 0.5$) to comply with the observed low abundance [^{24}Mg/Fe] in M 13 giants; *(ii)* it seems to disagree with the approximate constancy of the sum C+N+O reported in several globular clusters (and noted in Sect. 1) because it assumes the initial abundance of C (and N) in low mass stars to be a function of the dilution coefficient q, which may change from star to star; *(iii)* and, unfortunately, there are still many uncertainties in this scenario which do not allow us to draw more definite conclusions.

We conclude this section by noting that our calculations of the s-process nucleosynthesis in the $5\,M_\odot$ AGB star with $Z = 10^{-4}$ (which are in excellent agreement with the earlier results of Busso et al. (1988)) show that there is no substantial production of neutron-addition nuclides. Hence, we do not expect that the increased initial ^{25}Mg abundance in GCRGs has to correlate with any enhancement of the s-process elements. At present s-process nucleosynthesis is believed to occur in low mass ($1 - 3\,M_\odot$) AGB stars where the neutron source reaction is ^{13}C(α,n)^{16}O rather than ^{22}Ne(α,n)^{25}Mg as in our case (Gallino et al. 1988). Therefore, the observational data of ND95 showing that in ω Cen giants abundances of some typical s-process elements (Y, Ba, La and Nd) rise as [Fe/H] increases was interpreted by them as evidence of primordial enrichment by $1 - 3\,M_\odot$ AGB stars. Or to reverse the argument, if one accepts that the s-process elements are enhanced in ω Cen by the ejecta of $1 - 3\,M_\odot$ AGB stars, it follows that this should be accompanied by overabundances of the heavy nuclides of Mg resulting from the ejecta of their $3 - 8\,M_\odot$ counterparts.

4.3. A "black box" solution

If the observed Al enhancements in red giants with depleted [Mg/Fe] in the clusters M 13 and ω Cen are in fact produced at the expense of ^{24}Mg and not ^{25}Mg and if nuclear physicists confirm the currently-accepted rate of the reaction ^{24}Mg(p,γ)^{25}Al, the only remaining explanation of the MgAl anticorrelation is hydrogen burning at much higher temperatures than those ($T_6 \leq 55$) found in the HBS in the standard evolutionary models.

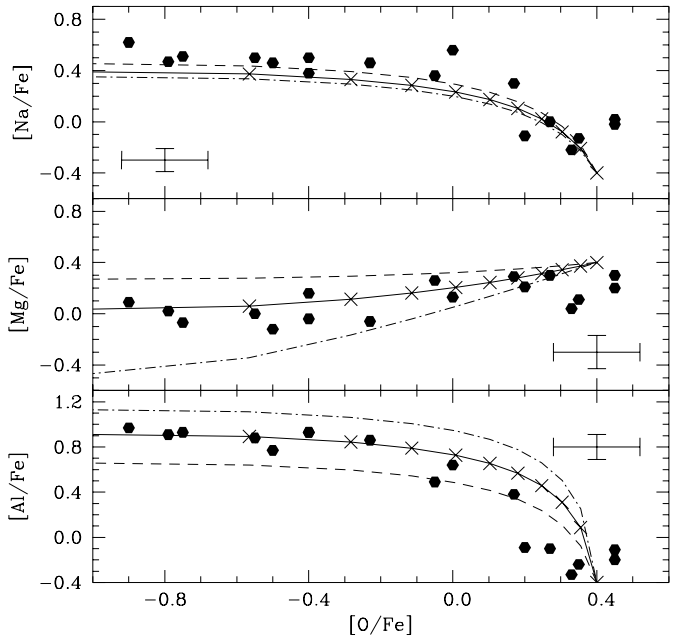

Fig. 8. Relations between the abundances of O, Na, Mg and Al (lines) in mixtures with the fraction of unprocessed material varied from 0% to 100% (crosses correspond to 100%, 90%, 80%,... from right to left). In the processed material hydrogen burning at constant density $\rho = 44.7\,\mathrm{g\,cm^{-3}}$ and temperature has been followed until 5% of H was consumed. The temperature has been adjusted ($T_6 = 70$ – short-dashed lines, $T_6 = 74$ – solid lines and $T_6 = 78$ – dot-short-dashed lines) to fit the correlations in M 13 giants (symbols). The initial chemical composition was that described in Sect. 3.1

To test this idea we have considered hydrogen burning at constant temperature and density. The density was chosen as $\rho = 44.7\,\mathrm{g\,cm^{-3}}$ as in the deep mixing study of Langer et al. (1993) and the initial chemical composition was that specified in Sect. 3.1. Nucleosynthesis calculations were interrupted when 5% of hydrogen was consumed. After that the calculated abundances were mixed with unprocessed material whose fraction was varied from 0% to 100%. Temperature was treated as a free parameter. The results are shown in Fig. 8 where the lines are the computed correlations between the final abundances of O, Na, Mg and Al. Crosses on the solid lines correspond (from right to left) to mixtures in which the fraction of unprocessed material is $q = 1.0, 0.9, 0.8, \ldots$(the last crosses seen on the left on the solid lines have $q = 0.1$). The range of temperatures fitting the anticorrelations of [O/Fe] versus [Na/Fe] and [Al/Fe] and the correlation of [O/Fe] versus [Mg/Fe] has turned out to be strikingly narrow: $T_6 = 70$ (short-dashed line), $T_6 = 74$ (solid line) and $T_6 = 78$ (dot-short-dashed line). Hence, were this idea right we could very precisely estimate the temperature of the hydrogen burning whose products are seen in GCRGs: $T_6 = 74 \pm 2$! The choice of density does not affect this estimate and if we take the amount of H to be consumed considerably different from 5% then it becomes more difficult to fit all three observed abundance correlations with the same value of temperature. It is interesting that a very similar result (with a slightly higher temperature $T_6 = 78$) is obtained when one considers hydrogen burning in a massive convective core (we have modelled the core structure with a polytrope $n = 1.5$ and this time the free parameter to adjust was the central temperature).

The next question to answer is which stellar environment may be identified with the "black box" described above. We calculated a ZAMS model of a $M = 125\,M_\odot$ star with $Z = 4\,10^{-4}$ but found that it had a central temperature $T_6 = 53$, which is too low. Any primordial origin of the hypothesized "black box" meets the difficulty of explaining why after consumption of only 5% of H the material was ejected into the intracluster medium. Another problem is understanding how some low mass stars succeeded in capturing as much as 90% of the material ejected by the "black box" (Fig. 8). These two problems are, however, easily solved if we place such a "black box" inside a star ascending the RGB, bearing in mind, of course, that we now have to think of a mechanism which can increase the temperature in the HBS up to the value $T_6 = 74$. Recently Langer et al. (1997) came to similar conclusions. They have proposed that it is the thermal instability of the HBS that causes episodical rises of the HBS temperature.

This having been said, the idea of a hot hydrogen burning origin of the MgAl anticorrelation in GCRGs also disagrees with the M 13 magnesium isotopic analysis of S96 because at $T_6 = 74$ not only ^{24}Mg but also ^{25}Mg and ^{26}Mg are quickly destroyed. For example, if we begin with the summed abundance [^{25}Mg+^{26}Mg/Fe] = 0 and isotopic ratios ^{24}Mg/^{25}Mg/^{26}Mg = 90/4.5/5.0 (corresponding to the chemical composition described in Sect. 3.1, and which are also very close to the ratios observed in the "unmixed" M 13 giant L598 of S96), then after consumption of 5% of H we find [^{25}Mg+^{26}Mg/Fe] = –0.50 (whereas Shetrone reported values as large as +0.21) and ^{24}Mg/^{25}Mg/^{26}Mg = 92.3/4.7/3.0 (in comparison with S96's average ratios 56/22/22). Is this an insuperable problem? A possible solution might be to postulate even higher initial abundances of the heavier Mg isotopes. What would certainly be most worthwhile is confirmation of the S96 result, and accurate data for a larger group of objects to more strongly constrain the situation.

5. Concluding remarks

We have shown that the hypothesis of deep mixing in stars ascending the RGB can explain self-consistently the anomalous abundances of C (as well as the ^{12}C/^{13}C ratios), N, O and Na in ω Cen giants and the global anticorrelation of [O/Fe] versus [Na/Fe] most clearly seen in M 13 giants. There is much other observational evidence of deep mixing in GCRGs, the most direct being the progressive decline of [C/Fe] with increasing luminosity on the RGB seen in several globular clusters (see references in Sect. 1). Similar evidence has been obtained recently by Pilachowski et al. (1996), who report that red giants in M 13 become more enriched in Na as they approach the RGB tip.

We did not discuss the nature of the mechanism driving the deep mixing. The most promising candidate seems to be some kind of rotationally induced instability (baroclinic and/or

shear instability etc.). In this case clusters with especially strong star-to-star abundance variations are expected to contain a lot of rapidly rotating stars. Indeed, horizontal branch stars in M 13 are found to possess unusually fast rotation (Peterson et al. 1995), and ω Cen seems to have one of the bluest horizontal branches among the globular clusters (Whitney et al. 1994) which may be a manifestation of surface He enrichment during RGB evolution (Rood 1973; Sweigart 1997). Of course, the latter observational fact does not exclude a primordial origin of any He enrichment.

Unfortunately, the deep mixing scenario alone cannot account for the MgAl anticorrelations in the M 13 and ω Cen giants in the absence of additional *ad hoc* assumptions. Possible modifications include a strong but still undetected low energy resonance in the reaction ^{24}Mg(p,γ)^{25}Al, and episodical increases of the HBS temperature up to the value $T_6 \approx 74$ (the standard models predict $T_6 \leq 55$) in stars ascending the giant branch. The first assumption, however, will most probably raise objections by nuclear physicists, whereas the second disagrees with the results of S96's magnesium isotopic analysis (Sect. 4.3). As regards the second possibility, the work of taking into account feedback from deep mixing on the structure and evolution of red giants still remains to be done before one can draw any further conclusions. Finally, given the importance of Shetrone's results for the present discussion, we emphasize the importance of their confirmation and amplification.

On the other hand, there are very convincing observational arguments in favour of the primordial scenario. To those mentioned in Sect. 4 one can add the well-known CN bimodality in 47 Tuc stars which has been traced down to the MS turn-off (Briley et al. 1994). Moreover, Briley et al. (1996) have recently shown that the strong CN (and weak CH) molecular band widths are accompanied by spectroscopic signatures of increased Na abundance in stars just below the MS turn-off in 47 Tuc. We have tried to determine whether mixing in a low mass MS star can produce surface C depletion accompanied by N and Na enhancements without dredging up too much He (which would conflict with the very narrow CM diagram of 47 Tuc at the MS turn-off; VandenBerg & Smith 1988), but we failed even with the new NeNa-cycle reaction rates of El Eid & Champagne (1995). Hence, the CN bimodality and the Na enhancements in 47 Tuc stars are most likely of primordial origin and AGB stars might be responsible for this.

We have proposed a primordial plus deep mixing scenario in which intermediate mass AGB stars are considered as the source of a primordial anticorrelation of ^{24}Mg versus ^{25}Mg in GCRGs, with ^{24}Mg being depleted in HBB, and ^{25}Mg being increased in He shell burning during pulses. The anticorrelations of [O/Fe] versus [Al/Fe] in M 13 and ω Cen giants are then very well reproduced in the deep mixing calculations with Al synthesized at the expense of ^{25}Mg. To produce extremely large Al enhancements, which are observed in some GCRGs, this scenario requires that the following two *necessary* conditions be fulfilled: (1) the star must have a high initial ^{25}Mg abundance, and (2) a deep mixing mechanism must be switched on in the star on the RGB.

An observational confirmation of our combined scenario would be finding a red giant which did not show signs of deep mixing (i.e. had large [O/Fe] and low [Na/Fe] and [Al/Fe]), but at the same time possessed depleted [Mg/Fe] and increased [^{25}Mg+^{26}Mg/Fe]. At present there is only one star in S96's sample, L598, showing no sign of efficient (if at all) mixing. Unfortunately, with ^{24}Mg/^{25}Mg/^{26}Mg = 94/3/3, it does not possess any trace of pollution from intermediate mass AGB stars. Hence, for this particular object both of the above conditions are not met. Another test would be to determine whether the sum ^{25}Mg+^{26}Mg in fact consists of ^{26}Mg only, because in our calculations the ^{25}Mg isotope is destroyed completely in GCRGs with efficient mixing.

We comment, finally, on the differences in the abundance patterns between globular cluster red giants, on the one hand, and the field halo giants, on the other. These groups differ in two well documented ways. First, anomalies involving C and N are much more prevalent in cluster stars (see Langer, Suntzeff & Kraft 1992, and references therein), and, second, it appears that enhancements of [(^{25}Mg+^{26}Mg)/^{24}Mg] exist preferentially in clusters rather than in the field. In the context of the two above-noted conditions, it appears that for field stars one would then require that neither of them be met. That is to say, one requires not only that field stars have not experienced enrichment from AGB stars but also that they have not experienced deep mixing. One might argue that economy of hypothesis suggests it is more palatable to assume, in the context of the alternatives discussed above, that an agency exists in globular cluster giants which leads both to deep mixing, on the one hand, and which operates in conjunction with either the postulated elevated temperatures ($T_6 = 74$) in the HBS or an accelerated rate for the reaction ^{24}Mg(p,γ)^{25}Al, on the other, and that this does not exist in the field stars.

Recently Smith & Kraft (1996) have considered another combined scenario where the initial overabundance of ^{25}Mg in GCRGs is assumed to come from Ne novae. Our paper extends the list of primordial plus deep mixing scenarios. What will be next?

Acknowledgements. P.A.D. wishes to express his gratitude for the warm hospitality of the staff of the Max-Planck-Institut für Astrophysik where the s-process nucleosynthesis code was prepared and appreciates the very favourable working atmosphere at the Mount Stromlo & Siding Spring Observatories where this study was carried out. P.A.D., G.S.Da C. and J.E.N. gratefully acknowledge financial support from the Department of Industry, Science & Tourism of the Australian Government, for a visit of P.A.D. to Australia, during which this work was performed. Our special thanks go to A.I.Boothroyd, J.C.Lattanzio, K.Takahashi, C.Tout and S.E.Woosley.

References

Alongi M., Bertelli G., Bressan A., Chiosi C., 1991, A&A 244, 95
Anders E., Grevesse N., 1989, Geochim. Cosmochim. Acta 53, 197
Arnould M., Mowlavi N., Champagne A., 1995, In: Noels A., et al. (eds.), Stellar Evolution: What Should Be Done, Univ. Liège, Liège, 17
Bao Z., Käppeler F., 1987 AD&NDT 36, 411

Beer H., Käppeler F., Arcoragi J.-P., 1989, In: Hillebrandt W., Müller E. (eds.), Proc. of the 5th Workshop on Nuclear Astrophysics, 10
Bell R.A., Dickens J.A., Gustafsson B., 1979, ApJ 229, 604
Boothroyd A.I., Sackmann I.-J., Wasserburg G.J., 1995, ApJ 442, L21
Briley M.M., Bell R.A., Hoban S., Dickens R.J., 1990, ApJ 359, 307
Briley M.M., Hesser J.E., Bell R.A., Bolte M., Smith G.H., 1994, AJ 108, 2183
Briley M.M., Smith V.V., Lambert D.L., 1994, ApJ 424, L119
Briley M.M., Smith V.V., Suntzeff N.B., et al., 1996, Nat 383, 604
Brown J.A., Wallerstein G., 1989, AJ 98, 1643
Brown J.A., Wallerstein G., 1993, AJ 106, 133
Brown J.A., Wallerstein G., Oke J.B., 1991a, AJ 101, 1693
Brown J.H., Burkert A., Truran J.W., 1991b, ApJ 376, 115
Brown J.H., Burkert A., Truran J.W., 1995, ApJ 440, 666
Busso M., Picchio G., Gallino R., Chieffi A., 1988, ApJ 326, 196
Carney B.W., 1996, In: Morrison H., Sarajedini A. (eds.), Formation of the Galactic Halo... Inside and Out, ASP Conference Series, Vol. 92, 103
Caughlan G.R., Fowler W.A., 1988, AD&NDT 40, 283 (CF88)
Cavallo R.M., Sweigart A.V., Bell R.A., 1996, ApJ 464, L79
Cavallo R.M., Sweigart A.V., Bell R.A., 1997, ApJ, accepted
Cayrel R., 1986, A&A 168, 81
Charbonnel C., 1994, A&A 282, 811
Charbonnel C., 1995, ApJ 453, L41
Cottrell P.L., Da Costa G.S., 1981, ApJ 245, L79
Cowan J.J., Thielemann F.-K., Truran J.W., 1991, Phys. Rep. 208, 267
Da Costa G.S., Cottrell P.L., 1980, ApJ 236, L83
Denissenkov P.A., 1990, Astrophysics 31, 588
Denissenkov P.A., Denissenkova S.N., 1990, SvA Lett. 16, 275
Denissenkov P.A., Weiss A., 1996, A&A 308, 773 (Paper I)
Denissenkov P.A., Weiss A., Wagenhuber J., 1997, A&A 320, 115 (Paper II)
Dickens R.J., Bell R.A., Gustafsson B., 1979, ApJ 232, 428
Dickens R.J., Croke B.F.W., Cannon R.D., Bell R.A., 1991, Nat 351, 212
El Eid M.F., Champagne A.E., 1995, ApJ 451, 298
Fowler W.A., Caughlan G.R., Zimmerman B.A., 1967, ARA&A 5, 525
Frost C.A., Lattanzio J.C., 1996, ApJ 473, 383
Gallino R., Busso M., Picchio G., Raiteri C.M., Renzini A., 1988, ApJ 334, L45
Gilroy K.K., Brown J.A., 1991, ApJ 371, 578
Haft M., Raffelt G., Weiss A., 1994, ApJ 425, 222
Holmes J.A., Woosley S.E., Fowler W.A., Zimmerman B.A., 1976, AD&NDT 18, 305
Iglesias C.A., Rogers F.J., 1996, ApJ 464, 943
Jura M., 1986, ApJ 301, 624
Kippenhahn R., 1974, In: Tayler R.J., Hesser J.E. (eds.), Late Stages of Stellar Evolution, Proc. of IAU Symp. 66, Dordrecht, Reidel, 20
Kraft R.P., 1994, PASP 106, 553
Kraft R.P., Sneden C., Langer G.E., Prosser C.F., 1993, AJ 104, 645
Kraft R.P., Sneden C., Smith G.H., et al., 1997, AJ 113, 279
Kudritzki R.P., Pauldrach A., Puls J., Voels S.R., 1991, In: Milne D., Haynes R. (eds.), The Magellanic Clouds, IAU Symp. 148, Kluwer Acad. Publ., 279
Laird J.B., Sneden C., 1996, In: Morrison H., Sarajedini A. (eds.), Formation of the Galactic Halo... Inside and Out, ASP Conference Series, Vol.92, 192
Landré V., Prantzos N., Aguer P., Bogaert G., Lefebvre A., Thibaud J.P., 1990, A&A 240, 85
Langer G.E., Hoffman R.D., 1995, PASP 107, 1177
Langer G.E., Kraft R.P., Carbon D.F., Friel E., Oke J.B., 1986, PASP 98, 473
Langer G.E., Hoffman R., Sneden C., 1993, PASP 105, 301
Langer G.E., Hoffman R.D., Zaidins C.S., 1997, PASP 109, 244
Langer G.E., Suntzeff N.B., Kraft R.P., 1992, PASP 104, 523
Lattanzio J.C., Frost C.A., 1997, The Asymptotic Giant Branch. In: Fundamental Stellar Properties: The Interaction Between Observation and Theory, Proc. IAU Symp. 189, in press
Lattanzio J.C., Frost C.A., Cannon R.C., Wood P.R., 1997, Nucleosynthesis in Intermediate Mass Stars. In: Wing R.F. (ed.), The Carbon Star Phenomenon, Proc. of IAU Symp. 177, in press
Maeder A., 1992, A&A 264, 105
McWilliam A., Lambert D.L., 1988, MNRAS 230, 573
Norris J., Cottrell P.L., 1979, ApJ 229, L69
Norris J.E., Da Costa G.S., 1995, ApJ 447, 680 (ND95)
Norris J., Freeman K.C., Cottrell P.L., Da Costa G.S., 1981, ApJ 244, 205
Paczyński B., 1970, Acta Astron. 20, 47
Paltoglou G., Norris J.E., 1989, ApJ 336, 185
Peterson R.C., Rood R.T., Crocker D.A., 1995, ApJ 453, 214
Pilachowski C.A., Sneden C., Kraft R.P., Langer G.E., 1996, AJ 112, 545
Raffelt G., Weiss A., 1992, A&A 264, 536
Ratynski, Käppeler F., 1988, Phys. Rev. C 37, 595
Renzini A., 1981, In: Iben I.Jr., Renzini A. (eds.), Physical Processes in Red Giants, Reidel, Dordrecht, 431
Renzini A., Voli M., 1981, A&A 94, 175
Rogers F.J., Iglesias C.A., 1992, ApJS 79, 507
Rood R.T., 1973, ApJ 184, 815
Sackmann I.-J., Boothroyd A.I., 1997, preprint astro-ph/9512122
Salpeter E.E., 1955, ApJ 121, 161
Schatz H., Jaag S., Linker G., et al., 1995, Phys. Rev. C 51, 379
Shetrone M.D., 1996a, AJ 112, 1517
Shetrone M.D., 1996b, AJ 112, 2639 (S96)
Shetrone M.D., 1997, Extreme Deep Mixing in Globular Cluster Giants: Constraint On Future Stellar Models. In: Fundamental Stellar Properties: The Interaction Between Observation and Theory, Proc. IAU Symp. 189, in press
Smith G.H., Kraft R.P., 1996, PASP 108, 344
Smith G.H., Tout C.A., 1992, MNRAS 256, 449
Smith G.H., Shetrone M.D., Bell R.A., Churchill C.W., Briley M.M., 1996, AJ 112, 1511
Smith V.V., Suntzeff N.B., 1989, AJ 97, 1699
Suntzeff N.B., Smith V.V., 1991, ApJ 381, 160
Sweigart A.V., 1997, ApJ 474, L23
Sweigart A.V., Mengel J.G., 1979, ApJ 229, 624
Takahashi K., Yokoi K., 1987, AD&NDT 36, 375
Talon S., Zahn J.-P., 1997, A&A 317, 749
Timmes F.X., Woosley S.E., Weaver T.A., 1995, ApJS 98, 617 (TWW95)
VandenBerg D.A., Smith G.H., 1988, PASP 100, 314
Wagenhuber J., Weiss A., 1994, A&A 290, 807
Walker T.P., Steigman G., Kang H.-S., Schramm D.M., Olive K.A., 1991, ApJ 376, 51
Weidemann V., 1987, A&A 188, 74
Weiss A., Wagenhuber J., Denissenkov P.A., 1996, A&A 313, 581
Wheeler J.C., Sneden C., Truran J.W., 1989, ARA&A 27, 279
Whitney J.H., O'Connell R.W., Rood R.T., et al., 1994, AJ 108, 1350
Woosley S.E., Weaver T.A., 1995, ApJS 101, 181
Woosley S.E., Fowler W.A., Holmes J.A., Zimmerman B.A., 1978, AD&NDT 22, 371
Zahn J.-P., 1992, A&A 265, 115
Zaidins C.S., Langer G.E., 1997, PASP 109, 252